

## Theory of Three-Photon Ionization of the Alkali Atoms\*

H. BARRY BEBB†

*Institute of Optics, University of Rochester, Rochester, New York*

(Received 5 August 1966)

Three-photon ionization transition rates are calculated for the alkali atoms (except Li) using quantum defect Coulomb functions to evaluate the well-known perturbation formula. Several corrections of previous work are mentioned. The often-used approximation of keeping only a small number of intermediate states is investigated. The predicted three-photon ionization rate (in cgs units) of the alkalis for the ruby photon energy of 1.78 eV is of the order of  $10^{-77} \times (\text{photon flux})^3$ . Detailed results are presented as dispersion curves of the transition rate for photon energies between the three-photon and two-photon thresholds.

### I. INTRODUCTION

THE alkali atoms (except lithium) ionize with the absorption of three ruby-laser photons. The ionization potentials of the heavier alkalis are low enough to permit three-photon ionization with Stokes-shifted ruby lines. These experimental conveniences have motivated calculations of the three-photon ionization rates for photon energies between the three-photon and two-photon thresholds. Recently, the two-photon ionization rates of the alkalis have been calculated<sup>1</sup> and, in conjunction with earlier work<sup>2</sup> on the one-photon ionization and the present work, theoretical predictions for the photoionization rates of the alkalis have been made available for photon energies between about one-third of the one-photon threshold to well above the one-photon threshold.

Even at a time when the details of the one-photon ionization of the alkalis are still under scrutiny,<sup>3</sup> Hall has investigated the two-photon ionization of Cs vapor using the second harmonic of ruby (and several Stokes-shifted second-harmonic lines), making careful comparisons between experiment and theory.<sup>4</sup> Yatsiv *et al.*<sup>5</sup> estimated the one-photon photo-ionization rate from the  $6s_{1/2}$  excited state of potassium which was saturated by a double quantum transition from the ground state. This calculation, which is almost incidental to their excellent work on double quantum saturation of an excited level, can be regarded as three-photon ionization in the case that one (or both) of the photons is in resonance with an intermediate state. Additional references and discussion can be found in Ref. 1.

### II. THEORY

In previous work, the theory of multiphoton ionization has been developed and applied to several systems.

\* Research supported in part by the U. S. Air Force Office of Scientific Research and in part by the U. S. Army Research Office, Durham, North Carolina.

† Present address: Texas Instruments Inc., Dallas, Texas.

<sup>1</sup> H. B. Bebb, *Phys. Rev.* **149**, 25 (1966).

<sup>2</sup> A. Burgess and J. J. Seaton, *Monthly Notices Roy. Astron. Soc.* **120**, 121 (1960).

<sup>3</sup> R. D. Hudson, *Phys. Rev.* **135**, A1212 (1964); R. D. Hudson and N. L. Carter, *ibid.* **137**, A1648 (1965); **139**, A1426 (1965).

<sup>4</sup> J. L. Hall, in *IEEE J. Quantum Electron.* **2**, No. 4, p. xxi (1966); also private communication.

<sup>5</sup> S. Yatsiv, W. G. Wagner, G. S. Picus, and F. McClung, *Phys. Rev. Letters* **15**, 614 (1965).

Careful calculations have been made for  $N$ -photon ionization of hydrogen<sup>6</sup> ( $N=2$  through 12) and for two-photon ionization of the alkali atoms.<sup>1</sup> More approximate treatments have been performed for the multiphoton ionization of the rare-gas atoms for ruby-laser light.<sup>6</sup> In this section some of the principal results of the afore-mentioned work are reviewed and then applied to three-photon ionization of the alkali atoms. Several minor corrections and clarifications of previous work are mentioned.

The integrated transition rate (in units of  $\text{sec}^{-1}$ ) for  $N$ -photon ionization is given by

$$w_{k,g}^{(N)} = 2\pi\hbar(2\pi\alpha F\omega)^N S^{(N)}(k; g), \quad (1a)$$

where

$$S^{(N)}(k; g) = \frac{\rho}{g_0} \sum_m \int d\Omega_k |\langle k | \tau^{(N)} | g \rangle|^2. \quad (1b)$$

Here  $\alpha$  is the fine-structure constant  $e^2/\hbar c$ ,  $F$  is the flux in  $\text{cm}^{-2} \text{sec}^{-1}$ , and  $\omega$  is the photon radial frequency. The set of quantum numbers specifying the ground state is denoted  $g$  and the continuum states are specified by the electron propagation vector  $\mathbf{k}$ . The degeneracy  $g_0$  of the ground state  $|g\rangle$  has been included in the definition of the "ionization strength"  $S^{(N)}(k; g)$ . The strength defined here might thus be regarded as the "average strength" rather than the "total strength" defined by Condon and Shortley.<sup>7</sup> The sum over  $m$  spans the  $g_0$  degenerate magnetic components of the ground state and often reduces to the factor  $g_0$ , just canceling the  $g_0$  in the denominator. The density of states  $\rho$  is included in the definition of  $S^{(N)}(k; g)$  to insure its independence of the normalization convention used for the continuum states. For the normalization convention used here,  $\rho = m\hbar k / (2\pi\hbar)^3$ .

The  $N$ th order transition operator  $\tau^{(N)}$  is defined

$$\tau^{(N)} = \left[ \prod_{\nu=1}^{N-1} \sum_{a_\nu} \frac{z | a_\nu \rangle \langle a_\nu |}{\omega_{a_\nu, g} - \nu\omega} \right] z, \quad (1c)$$

<sup>6</sup> (a) H. B. Bebb and A. Gold, *Phys. Rev.* **143**, 1 (1966); (b) also see *Physics of Quantum Electronics*, edited by P. L. Kelley, B. Lax, and P. E. Tannenwald (McGraw-Hill Book Company, New York, 1966), p. 489.

<sup>7</sup> E. U. Condon and G. H. Shortley, *The Theory of Atomic Spectra* (Cambridge University Press, London, 1959).

where the sums over the intermediate states  $a$ , include complete sets of states discrete plus continuum. The quantity  $\langle \mathbf{k} | \tau^{(N)} | g \rangle$  is seen to be just the usual  $N$ th-order matrix element.

For many atomic systems, the final-state continuum functions can to a good approximation be taken as Coulomb functions in the partial-wave expansion<sup>2,8</sup>

$$|\mathbf{k}\rangle = 4\pi \sum_{m_s} \sum_l \sum_{m_l} i^l e^{i\eta_l} Y_l^{m_l}(\theta, \phi) |k, l, m_l, m_s\rangle, \quad (2a)$$

where

$$|k, l, m_l, m_s\rangle = R_l(k, r) Y_l^{m_l}(\theta, \phi) \chi(m_s). \quad (2b)$$

The radial function  $R_l(k, r)$  is normalized so that it asymptotically approaches

$$R_l(k, r) \underset{kr \rightarrow \infty}{\sim} (kr)^{-1} \sin(x + \delta(k^2)), \quad (3a)$$

where

$$x = kr + k^{-1} \ln(2kr) - \frac{1}{2}l\pi + \eta_l. \quad (3b)$$

The phase  $\delta(k^2)$  accounts for the "quantum-defect" distortion of the continuum functions and vanishes as the quantum defect goes to zero.<sup>2</sup>

For definiteness, we specify the ground state  $|g\rangle$  in the  $jm$  representation by  $|nljm\rangle$ . Substituting Eq. (2a) into Eq. (1b), the ionization strength reduces to

$$S^{(N)}(k; nlj) = \frac{\rho(4\pi)^2}{2j+1} \sum_{m=-j}^j \sum_{l' m_l' m_s'} |\langle k l' m_l' m_s' | \tau^{(N)} | nljm \rangle|^2 \quad (4)$$

after some straightforward algebra. Here,  $g_0$  is replaced by its definition  $2j+1$ .

We now specialize to three-photon ionization explicitly writing out the third-order matrix element using the  $jm$  eigenstates for the intermediate states,

$$S^{(3)}(k; nlj) = \frac{\rho(4\pi)^2}{2j+1} \sum_{m=-j}^j \sum_{l' m_l' m_s'} \left| \sum_{(nljm)_1} \sum_{(nljm)_2} \frac{\langle k l' m_l' m_s' | z | (nljm)_2 \rangle \langle (nljm)_2 | z | (nljm)_1 \rangle \langle (nljm)_1 | z | nljm \rangle}{\Omega(nlj)_2 \Omega(nlj)_1} \right|^2. \quad (5)$$

The energy denominators do not depend on the magnetic quantum number  $m$  and are completely specified by the quantum numbers  $(nlj)$  with the notation

$$\hbar\Omega(nlj)_\nu = \epsilon(nl_\nu j_\nu) - \epsilon(nlj) - \nu\hbar\omega.$$

Here,  $\hbar\omega$  is the photon energy,  $\epsilon(nlj)$  is the ground-state energy, and  $\epsilon(nl_\nu j_\nu)$  is the energy of the  $\nu$ th intermediate state. In Eq. (5) we have also adopted a convention of using subscripted parentheses to indicate a set of variables with a common subscript, i.e.,  $(nljm)_\nu \equiv n, l_\nu, j_\nu, m_\nu$ .

While the reduction of Eq. (5) to a computational form is quite straightforward, the algebraic steps required are tedious and numerous. Rather than pursuing this cumbersome and unrewarding task with elaborate generality, we restrict our attention to one-electron atoms with  $s$  ground states and incorporate selection rules appropriate to the dipolar matrix elements, thereby simplifying Eq. (5) to

$$S^{(3)}(k; ns\frac{1}{2}) = \frac{\rho(4\pi)^2}{2j+1} \sum_{m=-j}^j \sum_{l' m_l' m_s'} \left| \sum_{(nlj)_2} \sum_{(nj)_1} \frac{\langle k l' m_l' m_s' | z | (nlj)_2 m \rangle \langle (nlj)_2 m | z | (npj)_1 m \rangle \langle (npj)_1 m | z | ns\frac{1}{2} m \rangle}{\Omega(nlj)_2 \Omega(npj)_1} \right|^2. \quad (6)$$

The  $jm$  functions are expanded into the  $m_l m_s$  functions via the Clebsch-Gordan series:

$$|nljm\rangle = \sum_{m_s} \langle l, s, m - m_s, m_s | jm \rangle |n, l, m - m_s, m_s\rangle, \quad (7)$$

where the condition  $m = m_l + m_s$  has been used. The angular-momentum quantum number  $l$  in the  $m_l m_s$  functions is subscripted with the associated  $j$  value as a reminder that the radial functions depend on  $j$  through the spin-orbit coupling.<sup>1</sup>

Using (7), the dipolar matrix elements appearing in Eq. (6) can be expressed in terms of dipolar matrix elements involving  $m_l m_s$  functions:

$$\langle (npj)_1 m | z | ns\frac{1}{2} m \rangle = \langle p\frac{1}{2} 0\frac{1}{2} | jm \rangle \langle (npj)_1 0 | z | ns_{1/2} 0 \rangle, \quad (8a)$$

$$\langle (nlj)_2 m | z | (npj)_1 m \rangle = \sum_{\nu=-1/2}^{1/2} \langle l_2, \frac{1}{2}, m - \nu, \nu | j_2 m \rangle \langle p, \frac{1}{2}, m - \nu, \nu | j_1 m \rangle \langle (nlj)_2 m | z | (npj)_1 m - \nu \rangle, \quad (8b)$$

and

$$\langle k, l', m - m_s', m_s' | z | (nlj)_2 m \rangle = \langle l_2, \frac{1}{2}, m - m_s, m_s | j_2 m \rangle \langle k, l', m - m_s | z | (nlj)_2 m - m_s \rangle. \quad (8c)$$

<sup>8</sup> H. B. Bebb, J. Math. Phys. 7, 957 (1966).

Substitution of (8) into (6) yields

$$S^{(3)}(k; n_s \frac{1}{2}) = \frac{\rho(4\pi)^2}{2j+1} \sum_{m=-j}^j \sum_{l', m_s'} \sum_{(nl_j)_2} \sum_{(n_j)_1} \sum_{\nu=-1/2}^{1/2} \left[ \langle l_2, \frac{1}{2}, m-m_s, m_s | j_2 m \rangle \langle l_2, \frac{1}{2}, m-\nu, \nu | j_2 m \rangle \langle p, \frac{1}{2}, m-\nu, \nu | j_1 m \rangle \right. \\ \left. \times \langle p, \frac{1}{2}, 0, \frac{1}{2} | j_1 m \rangle \right] \frac{\langle k, l', m-m_s' | z | (nl_j)_2 m-m_s' \rangle \langle (nl_j)_2 m-\nu | z | (np_j)_1 m-\nu \rangle \langle (np_j)_1 0 | z | n_s \frac{1}{2} 0 \rangle}{\Omega(nl_j)_2 \Omega(np_j)_1} \Big|^2. \quad (9)$$

This expression can be regarded as the computational formula for the ionization strength. While it appears formidable, its interpretation is obvious and its evaluation is easily affected with the aid of a digital computer. For those preferring less reliance on large computers, the result can be further reduced to an expression involving only dipole matrix elements by evaluating the Clebsch-Gordan coefficients and explicitly writing out the terms indicated by the summations:

$$S^{(3)}(k; n_s \frac{1}{2}) = \frac{m\hbar k}{(2\pi\hbar)^3} (4\pi)^2 \left[ \sum_{n'n} \left\{ \frac{1}{3} \frac{\langle kp | z | n' s_{1/2} \rangle \langle n' s_{1/2} | z | np_{1/2} \rangle \langle np_{1/2} | z | n_s s_{1/2} \rangle}{\Omega(n' s_{1/2}) \Omega(np_{1/2})} \right. \right. \\ \left. \left. + \frac{2}{3} \frac{\langle kp | z | n' s_{1/2} \rangle \langle n' s_{1/2} | z | np_{3/2} \rangle \langle np_{3/2} | z | n_s s_{1/2} \rangle + \frac{1}{3} \frac{\langle kp | z | n' d_{3/2} \rangle \langle n' d_{3/2} | z | np_{1/2} \rangle}{\Omega(n' d_{3/2}) \Omega(np_{1/2})} \right. \right. \\ \left. \left. \times \langle np_{1/2} | z | n_s s_{1/2} \rangle + \frac{1/15}{\Omega(n' d_{3/2}) \Omega(np_{3/2})} \langle kp | z | n' d_{3/2} \rangle \langle n' d_{3/2} | z | np_{3/2} \rangle \langle np_{3/2} | z | n_s s_{1/2} \rangle + \frac{9/15}{\Omega(n' d_{5/2}) \Omega(np_{3/2})} \langle kp | z | n' d_{5/2} \rangle \right. \right. \\ \left. \left. \times \langle n' d_{5/2} | z | np_{3/2} \rangle \langle np_{3/2} | z | n_s s_{1/2} \rangle \right\}^2 + \left| \sum_{n'n} \left\{ \frac{1}{3} \frac{\langle kf | z | n' d_{3/2} \rangle \langle n' d_{3/2} | z | np_{1/2} \rangle \langle np_{1/2} | z | n_s s_{1/2} \rangle}{\Omega(n' d_{3/2}) \Omega(np_{1/2})} \right. \right. \\ \left. \left. + \frac{1/15}{\Omega(n' d_{3/2}) \Omega(np_{3/2})} \langle kf | z | n' d_{3/2} \rangle \langle n' d_{3/2} | z | np_{3/2} \rangle \langle np_{3/2} | z | n_s s_{1/2} \rangle + \frac{9/15}{\Omega(n' d_{5/2}) \Omega(np_{3/2})} \langle kf | z | n' d_{5/2} \rangle \langle n' d_{5/2} | z | np_{3/2} \rangle \right. \right. \\ \left. \left. \times \langle np_{3/2} | z | n_s s_{1/2} \rangle \right\}^2 + \left| \sqrt{\frac{3}{4}} \sum_{n'n} \left\{ \frac{-(5\sqrt{6})/30}{\Omega(n' d_{3/2}) \Omega(np_{1/2})} \langle kp | z | n' d_{3/2} \rangle \langle n' d_{3/2} | z | np_{1/2} \rangle \langle np_{1/2} | z | n_s s_{1/2} \rangle + \frac{-(\sqrt{6})/30}{\Omega(n' d_{3/2}) \Omega(np_{3/2})} \right. \right. \\ \left. \left. \times \langle kp | z | n' d_{3/2} \rangle \langle n' d_{3/2} | z | np_{3/2} \rangle \langle np_{3/2} | z | n_s s_{1/2} \rangle + \frac{(6\sqrt{6})/30}{\Omega(n' d_{5/2}) \Omega(np_{3/2})} \langle kp | z | n' d_{5/2} \rangle \langle n' d_{5/2} | z | np_{3/2} \rangle \langle np_{3/2} | z | n_s s_{1/2} \rangle \right\}^2 \right. \\ \left. \left. + \left| \sqrt{\frac{3}{4}} \sum_{n'n} \left\{ \frac{-(5\sqrt{6})/30}{\Omega(n' d_{3/2}) \Omega(np_{1/2})} \langle kf | z | n' d_{3/2} \rangle \langle n' d_{3/2} | z | np_{1/2} \rangle \langle np_{1/2} | z | n_s s_{1/2} \rangle + \frac{-(\sqrt{6})/30}{\Omega(n' d_{3/2}) \Omega(np_{3/2})} \right. \right. \right. \\ \left. \left. \times \langle n' d_{3/2} | z | np_{3/2} \rangle \langle np_{3/2} | z | n_s s_{1/2} \rangle + \frac{(6\sqrt{6})/30}{\Omega(n' d_{5/2}) \Omega(np_{3/2})} \langle kf | z | n' d_{5/2} \rangle \langle n' d_{5/2} | z | np_{3/2} \rangle \langle np_{3/2} | z | n_s s_{1/2} \rangle \right\}^2 \right. \Big|^2. \quad (10)$$

The three-photon ionization rate is given by substituting Eq. (10) into Eq. (1a).

Angular integrals in (9) involving  $m_l = \pm 1$  have been expressed in terms of  $m_l = 0$  angular integrals in (10). Hence, the dipolar integrals appearing in (10) are all of the form

$$\langle n' l_j' | z | n l_j \rangle = \int R_{n' l_j'}(r) Y_{l_j'}^0(\theta, \phi) z R_{n l_j}(r) \\ \times Y_{l_j}^0(\theta, \phi) r^2 dr d\Omega. \quad (11)$$

Several comments about Eq. (10) are appropriate. First, the result is somewhat different from what would

be obtained by deriving selection rules based on the concept of average-energy denominators developed in Ref. 1. In particular, the last two terms (here we are regarding the set of elements enclosed in absolute-value signs as a term—there are four terms) which originate from  $m_l = \pm 1$  continuum functions would not appear.<sup>9</sup> This difference arises because  $\tau^{(3)}$  can be regarded as an operator transforming as  $z^3$  only in the space spanned by the true eigenfunctions of the Hamiltonian—in the present instance, the  $jm$  functions. However, in using approximate  $mm_s$  continuum functions, we have extended the space (i.e.,  $mm_s$  functions are not eigen-

<sup>9</sup> See note added in proof of Ref. 1.

functions of the complete Hamiltonian with spin-orbit coupling) and the result that  $\tau^{(3)}$  transforms as  $z^3$  is no longer strictly valid. On the other hand, the last two terms are almost always small compared with the first two, so that results based on average energies still provide an excellent approximation.

Second, as an instructive check on the result, consider the reduction of Eq. (10) as the spin-orbit energy

$$S^{(3)}(k; n_0s) = (m\hbar k / (2\pi\hbar)^3) (4\pi)^2 \left| \sum_{n'n} \left\{ \frac{1}{\Omega(n's)\Omega(np)} \langle kp|z|n's\rangle \langle n's|z|np\rangle \langle np|z|n_0s\rangle \right. \right. \\ \left. \left. + \frac{1}{\Omega(n'd)\Omega(np)} \langle kp|z|n'd\rangle \langle n'd|z|np\rangle \langle np|z|n_0s\rangle \right\}^2 + \left| \sum_{n'n} \frac{1}{\Omega(n'd)\Omega(np)} \langle kf|z|n'd\rangle \langle n'd|z|np\rangle \langle np|z|n_0s\rangle \right|^2 \right|. \quad (12)$$

Equation (12) is just a special case of the more general result given by Eqs. (39) and (40) of Ref. 6(a).<sup>10</sup>

### III. RESULTS AND DISCUSSION

The three-photon ionization strengths, Eq. (10), and the corresponding transition rates are estimated by replacing the infinite sums over intermediate states with a limited number of significant terms. The sum over first-order intermediate states  $|np_j\rangle$  is dominated by the lowest lying configuration due simultaneously to the large value of the corresponding matrix element

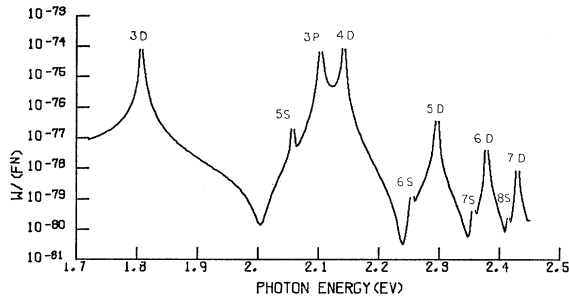


FIG. 1. Three-photon ionization rate of Na. The sum over the second-order intermediate  $s$  and  $d$  states extends to  $n'=9$ . The doublet structure of the  $3p$  and  $n'd$  levels is included in the computation but is not resolved in the dispersion curve. The symbol  $W/(F^3)$  should be interpreted as  $w_{k,\theta}^{(3)}/F^3$ .

<sup>10</sup> Equations (40), (41), and (42) of Ref. 6 contain an error. In the notation of Ref. 6, Eq. (40) should read

$$|\langle k|\tau^{(N)}|n_0l_0\rangle|^2 \\ = (4\pi)^2 \sum_{l=0}^{\infty} |\langle kl|\tau^{(N)}|n_0l_0\rangle|^2 \\ = (4\pi)^2 \sum_{l=0}^{\infty} \left\{ \sum_n \frac{\langle k,l|z|n,l+1\rangle}{(\omega_{n,n_0} - (N-1)\omega + i\gamma/2)} \right. \\ \left. \times \langle n,l+1|\tau^{(N-1)}|n_0l_0\rangle + \text{term in } (l-1) \right\}^2.$$

Analogous replacements should be made in Eqs. (41) and (42) of that work. The error resulted from an effort to simplify the notation. The correct expression as quoted here was actually used in the computations.

is "turned off." Results appropriate to  $m_l m_s$  functions should be recovered. As the spin-orbit coupling becomes negligible, frequencies associated with the same configuration but different  $j$  values collapse,  $\Omega(np\frac{1}{2}) = \Omega(np\frac{3}{2}) = \Omega(np)$ , and  $\Omega(nd\frac{3}{2}) = \Omega(nd\frac{5}{2}) = \Omega(nd)$ . The corresponding radial matrix elements also become independent of  $j$ . Thus, the last two terms vanish and the first two add to give

$\langle n=n_0, p_j|z|n_0s_{1,2}\rangle$  and the occurrence of a near resonance of the photon energy with the  $(n_0, p)$  configuration making  $\Omega(np_j)$  small. The summation over the second-order intermediate states is extended to include all  $(n's)$  and  $(n'd)$  configurations with energies that occur in resonance with  $2\hbar\omega$ . The contribution from the higher lying  $(np)$  and  $(n's)$ ,  $(n'd)$  configurations are discussed later.

The techniques used to evaluate the required dipolar matrix elements are detailed in Ref. 1. Briefly, the wave functions (for both the bound and free states) are approximated by quantum defect Coulomb functions and the radial integrals are calculated using the techniques of Bates and Damgaard<sup>11</sup> for the bound-bound integrals and the results of Burgess and Seaton<sup>2</sup> for the bound-free integrals.

A FORTRAN computer program was written to evaluate the three-photon ionization rate. The output from the IBM 7074 (the transition rate  $w_{k,\theta}^{(3)}$  and the photon energy  $\hbar\omega$ ) is written on magnetic tape which is used

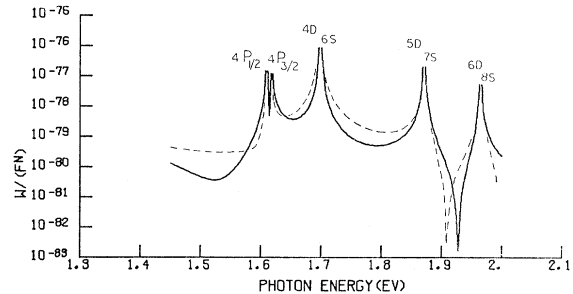


FIG. 2. Three-photon ionization rate of K. The sum over the second-order intermediate  $s$  and  $d$  states extends to  $n'=8$ . The sum over the first-order intermediate  $p$  states includes  $4p$  and  $5p$ . Only  $4p$  is near resonant within the photon energy range indicated. The doublet structure is clearly visible. The dashed line gives the results when the contribution from the  $5p$  intermediate state is neglected. Incorporating the higher  $p$  states than the  $5p$  state, on the other hand, does not affect the result indicated with the solid line. Note that the  $(n'+2, s)$  levels almost coincide with the  $(n', d)$  levels.

<sup>11</sup> D. R. Bates and A. Damgaard, Phil. Trans. Roy. Soc. London A242, 101 (1949).

as input for a Calcomp digital plotter. The digital plotter draws the transition rate as a function of photon energy. The dispersion curves, Figs. 1 through 4, are, reproduced directly from the digital-plotter output [the label  $W/(F^N)$  on the ordinate should be read as  $w_{k,g}^{(3)}/F^3$ ].

The three-photon ionization-rate dispersion curves for the alkalis Na, K, Rb, and Cs are given in Figs. 1-4 for photon energies between the three- and two-photon thresholds. The peaks arise from near resonances in both first and second order. The lowest lying  $p$  configuration shows a near resonance with  $\hbar\omega$  (first order), while the  $s$  and  $d$  configurations show near-resonances with  $2\hbar\omega$ . The occurrence of simultaneous near-resonances in first and second order leads to unusually large transition rates ( $w^{(3)} \sim 10^{-71} F^3$ ) in Rb and Cs for photon energies around 1.58 eV and 1.38 eV, respectively. For these photon energies, the three-photon ionization can to a good approximation be regarded as a sequence of three first-order transitions, say  $5s \rightarrow 5p_{3/2}$ ,  $5p_{3/2} \rightarrow 5d$ , and  $5d \rightarrow k$  for rubidium.

As previously implied, the often used approximation of replacing the infinite sums over intermediate states by a limited number of dominant terms was investigated by observing the change in the dispersion curve as the number of terms is increased. Of course, the terms occurring in near-resonance with the photon energy are clearly essential and should provide the major contribution near the corresponding peaks. Less obvious is the contribution of the nonresonant terms (including the continuum) to the valleys. The sum over first-order intermediate states is well approximated by keeping only the lowest two configurations coupling the ground state,  $(n_0, p)$  and  $(n_0+1, p)$ . The corresponding results with only the lowest configuration  $(n_0, p)$  are indicated by the dashed lines in Figs. 1-4. Only the transition rate of potassium obtains a significant contribution from the  $(n_0+1, p)$  configuration with a slight contribution occurring for rubidium and a negligible contribution for sodium or cesium. Higher

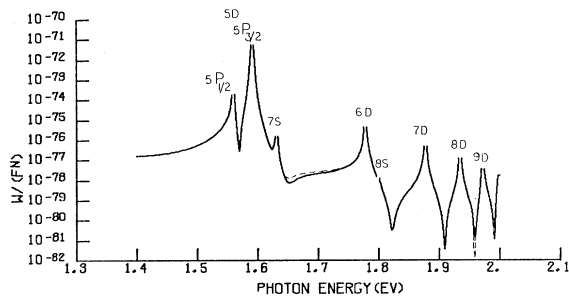


FIG. 3. Three-photon ionization rate of Rb. The sum over  $n'$  extends to  $n'=12$ . The enormous peak at 1.58 eV is due to simultaneous resonances occurring in first and second order. The  $s$  states above  $n'=8$  begin to coincide with the  $d$  states [e.g.,  $\epsilon(10,s)=3.887$  eV and  $\epsilon(8,d_{3/2})=3.870$  eV] are not resolved. The dashed line corresponds to approximating the sum over  $np$  by  $5p$ . The higher  $p$  states clearly contribute very little to the transition rate.

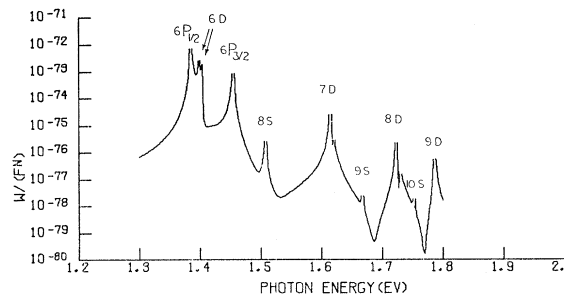


FIG. 4. Three-photon ionization rate of Cs. The sum over  $n'$  extends to  $n'=11$ . The splitting of the  $d$  lines as well as the  $p$  lines is sufficient in cesium to be resolved in the graph.

lying  $p$  configurations are certainly negligible. The sum over the second-order intermediate  $s$  and  $d$  states is well approximated by keeping only the near-resonant terms indicated in Figs. 1-4. However, it should be pointed out that more states than those labeled in the figures were actually used in the computations. They are indicated in the figure captions.

From the above arguments, the contribution from the continuum cannot be precluded as negligible. However, since the main part of the oscillator strengths of the relevant levels is provided by the discrete portion of the spectrum, we might expect the continuum contribution to the intermediate-state sums (in the perturbation formulas) to be small. This is certainly the case the case for the first-order intermediate states ( $np$ ), as argued in Ref. 1, but is less clear for the second-order summation over  $n'$ . Regardless, the continuum contribution can be significant only with respect to the deepest part of the valleys. We caution, however, that the deep valleys arise from cancellation effects between terms which can cause the transition rate to actually go to zero. A small contribution can shift the position of the minimum as well as the depth of the valley (for example, see Fig. 2). On the other hand, the results presented in Figs. 1-4 should be quantitatively reliable for most photon energies with uncertainties arising only near the deepest portions of the valleys.

#### IV. GAS BREAKDOWN

Recently, there has been considerable speculation about the role of multiple-photon ionization in the gas discharges observed at the focal region of  $Q$ -spoiled ruby and neodymium lasers.<sup>12</sup> The breakdown is conveniently divided into three states: initiation, growth, and recombination. The growth of the optical discharges in the rare gases appears to be accounted for by cascade ionization processes taking place through the agency of "free" electrons (in the neighborhood of gas atoms) absorbing energy from the optical field. Owing to the large ionization potential of the rare gases, multiple-

<sup>12</sup> C. S. Naiman, M. Y. DeWolf, I. Goldblatt, and J. Schwartz, Phys. Rev. **146**, 133 (1966). This article contains extensive references to the literature on gas breakdown.

photon ionization occurs with reasonably low probability and thus contributes significantly only to the initiation stage (at least at moderate pressures—say, around one atmosphere). At lower pressures,  $N$ -photon ionization should contribute in increasing amounts to the growth of the discharge due to its relative weak pressure dependence compared to cascade ionization processes (see, for example, Fig. 20 of Ref. 6).

The photon flux  $F$  (photons  $\text{cm}^{-2} \text{sec}^{-1}$ ) required to produce a given transition rate  $W$  (transitions  $\text{cm}^{-3} \text{sec}^{-1}$ ) is given by

$$F = N_0^{-1/N} (W/\delta^{(N)})^{1/N}, \quad (13)$$

where  $N_0$  is the atomic number density (roughly proportional to pressure) and  $w^{(N)} = \delta^{(N)} F^N$  is the transition rate per atom. For low-order processes—say,  $N=2$

or 3 (as appropriate for photo-ionization of the alkali gases with ruby laser light)—the flux required to produce a substantial transition rate  $W$  is significantly lower than for the higher order processes appropriate to the rare gases. Also, the pressure dependence for the lower order processes is much stronger, in accordance with Eq. (13). Hence, multiple-photon ionization should play a more dominant role (over appreciable pressure ranges) in the growth of gas discharges in the alkali gases than in the rare gases. The alkali gases thus seem to be interesting candidates for gas-breakdown experiments as well as for direct photo-ionization experiments.

#### ACKNOWLEDGMENTS

The author expresses his appreciation to Professor A. Gold and to J. O'Brien for several helpful discussions.

## Electron Photodetachment from $\text{O}^-$ and Elastic Scattering from Atomic Oxygen

W. R. GARRETT\*

*University of Alabama, Department of Physics and Research Institute, Huntsville, Alabama*

AND

H. T. JACKSON, JR.

*U. S. Army Missile Command, Research and Development Directorate, Redstone Arsenal, Alabama*

(Received 15 August 1966)

Cross sections have been determined for the photodetachment of an electron from the negative atomic-oxygen ion. Calculations are made for the three transitions  $\text{O}^{-2}P$  to  $\text{O}^3P$ ,  $\text{O}^1D$ , and  $\text{O}^1S$  with photon energies from threshold to 13.6 eV. A method is used wherein wave functions for both bound-state and continuum electrons are obtained through a modified version of Slater's approximation to the Hartree-Fock equations. Correlation effects are included through a polarization potential obtained from an application of first-order perturbation theory to the Hartree-Fock atomic system. Results are compared with the experiments of Smith and of Branscomb, Smith, and Tisone, giving very good low-energy agreement. In addition, the elastic-scattering cross section for neutral oxygen, the dipole polarizability, the attachment cross section, and attachment coefficient for electron capture were also determined. Agreement is quite good between these observables and available experimental data.

### I. INTRODUCTION

BECAUSE of their importance in terrestrial and stellar atmospheres, the cross sections for photodetachment of the negative atomic-oxygen ion and cross sections for low-energy electron scattering by atomic oxygen have been studied by a number of investigators both experimentally and theoretically.<sup>1</sup> In treating either of these problems theoretically there is the usual difficulty of adequately describing the continuum solutions at low energies, the ordinary Hartree-Fock treatment being inadequate because of correlation effects. In the case of the negative ion there is the added

problem of obtaining acceptable wave functions for the initial negative-ion state since, again because of neglect of correlation, Hartree-Fock solutions are not particularly accurate.

In the present treatment of these problems, a method is utilized wherein the bound-state system is described through a modification of the Hartree-Fock-Slater (HFS) technique and correlation effects are determined by a polarization potential obtained from the perturbation of the bound-state system by the detached (or scattered) electron. The latter has been applied with some success in low-energy electron scattering from alkali atoms<sup>2</sup> where polarization terms in the interaction potential are quite large.

\* Present address: Health Physics Division, Oak Ridge National Laboratory, Oak Ridge, Tennessee.

<sup>1</sup> See review by L. M. Branscomb, in *Atomic and Molecular Processes*, edited by D. R. Bates (Academic Press Inc., New York, 1962), p. 100.

<sup>2</sup> W. R. Garrett, *Phys. Rev.* **140**, A705 (1965); hereafter referred to as I.